

# The apolipoprotein A-I mimetic peptide, D-4F, restrains neointimal formation through heme oxygenase-1 up-regulation

Donghui Liu<sup>a, # \* </sup>, Mengzhang Wu<sup>a, b, #</sup>, Qian Du<sup>a, #</sup>, Zhenzhen Ding<sup>a, b</sup>, Mingming Qian<sup>a</sup>, Zijia Tong<sup>a, b</sup>, Wenqi Xu<sup>c</sup>, Le Zhang<sup>a</sup>, He Chang<sup>a</sup>, Yan Wang<sup>a</sup>, Caihua Huang<sup>d</sup>, Donghai Lin<sup>c</sup>

<sup>a</sup> Department of Cardiology, The Affiliated Cardiovascular Hospital of Xiamen University, Medical College of Xiamen University, Xiamen, China

<sup>b</sup> Union Clinical Medical College of Fujian Medical University, Fuzhou, China

<sup>c</sup> High-field NMR Research Center, MOE Key Laboratory of Spectrochemical Analysis & Instrumentation, College of Chemistry and Chemical Engineering, Xiamen University, Xiamen, China

<sup>d</sup> Department of Physical Education, Xiamen University of Technology, Xiamen, China

Received: November 13, 2016; Accepted: May 27, 2017

## Abstract

D-4F, an apolipoprotein A-I (apoA-I) mimetic peptide, possesses distinctly anti-atherogenic effects. However, the biological functions and mechanisms of D-4F on the hyperplasia of vascular smooth muscle cells (VSMCs) remain unclear. This study aimed to determine its roles in the proliferation and migration of VSMCs. *In vitro*, D-4F inhibited VSMC proliferation and migration induced by ox-LDL in a dose-dependent manner. D-4F up-regulated heme oxygenase-1 (HO-1) expression in VSMCs, and the PI3K/Akt/AMP-activated protein kinase (AMPK) pathway was involved in these processes. HO-1 down-regulation with siRNA or inhibition with zinc protoporphyrin (Znpp) impaired the protective effects of D-4F on the oxidative stress and the proliferation and migration of VSMCs. Moreover, down-regulation of ATP-binding cassette transporter A1 (ABCA1) abolished the activation of Akt and AMPK, the up-regulation of HO-1 and the anti-oxidative effects of D-4F. *In vivo*, D-4F restrained neointimal formation and oxidative stress of carotid arteries in balloon-injured Sprague Dawley rats. And inhibition of HO-1 with Znpp decreased the inhibitory effects of D-4F on neointimal formation and ROS production in arteries. In conclusion, D-4F inhibited VSMC proliferation and migration *in vitro* and neointimal formation *in vivo* through HO-1 up-regulation, which provided a novel prophylactic and therapeutic strategy for anti-restenosis of arteries.

**Keywords:** apoA-I mimetic peptide • vascular smooth muscle cell • HO-1 • proliferation • migration

## Introduction

Many factors are involved in the initiation and progression of atherosclerotic cardiovascular diseases (ASCVD) [1]. Arterial intimal hyperplasia is a prevalent pathophysiological process that contributes to atherosclerogenesis and in-stent restenosis [2]. In stress conditions, vascular smooth muscle cells (VSMCs) shift from a quiescent/contractile phenotype to an active/synthetic phenotype, which proliferate and migrate from the medial layer of vessels into the intima, resulting in neointimal hyperplasia and artery stenosis [3, 4]. Therefore, the efficient strategies aiming to inhibit neointimal formation would prevent the development of atherosclerotic plaque.

Oxidative stress is implicated in the formation of atherosclerotic lesions [5, 6]. Angiotensin II (ang-II) induces reactive oxygen species (ROS) generation and subsequently promotes VSMC proliferation and migration through ERK1/2 and p38 MAPK pathway [7]. Furthermore, increased plasma S-adenosyl-homocysteine induces VSMC proliferation and migration through oxidative stress-dependent ERK1/2 activation in apoE null mice [8]. However, overexpression of manganese superoxide dismutase (MnSOD) scavenges ROS, attenuates VSMC proliferation and migration, and suppresses neointimal formation [9]. Thus, inhibition of oxidative stress could alleviate neointimal formation [10].

High-density lipoprotein (HDL) provides important protections against atherogenesis, including promoting reverse cholesterol transport (RCT), improving endothelial cell functions, inhibiting inflammatory factor release and suppressing oxidative stress [11]. In addition,

#D.L., M.W. and Q.D. contributed equally to this work.

\*Correspondence to: Dr. Donghui LIU

E-mail: liudh@xmu.edu.cn

doi: 10.1111/jcmm.13290

© 2017 The Authors.

Journal of Cellular and Molecular Medicine published by John Wiley & Sons Ltd and Foundation for Cellular and Molecular Medicine.

This is an open access article under the terms of the Creative Commons Attribution License, which permits use, distribution and reproduction in any medium, provided the original work is properly cited.

HDL strikingly reduces the proliferation of VSMCs and prevents the pathogenesis of neointimal hyperplasia [12]. Decreased HDL levels in endothelial lipase (EL)-transgenic mice increase oxidative stress and promote neointimal formation in carotid arteries [13].

Apolipoprotein A-I (apoA-I) is the major apolipoprotein of HDL and exerts many anti-atherogenic effects, which makes it to be an attractive candidate for ASCVD treatment [14]. D-4F is a synthesized apoA-I mimetic peptide with 18 D-amino acids, which mimics the amphipathic helices of apoA-I and displays the biological features of native apoA-I [15]. D-4F inhibits atherosclerogenesis by decreasing plasma long-chain lysophosphatidylcholine (LysoPC) in low-density lipoprotein receptor (LDL-R) null mice [16]. In addition, D-4F induces nitric oxide (NO) biosynthesis, decreases ROS production and protects against myocardial infarction [17]. Besides, D-4F effectively protects endothelial cells against oxidized LDL (ox-LDL)-induced oxidative stress by preventing the down-regulation of pigment epithelium-derived factor (PEDF) [18]. Reverse D-4F inhibits neointimal formation, local neutrophil and macrophage infiltration, and monocyte chemotactic protein-1 (MCP-1) expression following carotid artery ligation in C57BL/6J mice [19]. However, the underlying mechanism for these effects remains unclear.

In this study, we demonstrated that D-4F suppressed VSMC proliferation and migration *in vitro* and inhibited neointimal formation of carotid arteries *in vivo* through up-regulating heme oxygenase-1 (HO-1) expression. PI3K/Akt and AMP-activated protein kinase (AMPK) were involved in the up-regulation of HO-1 induced by D-4F. And ATP-binding cassette transporter A1 (ABCA1) displayed significant effects in these processes. These results implied that D-4F might be a potential agent to prevent and treat artery restenosis.

## Materials and methods

### Materials

The antibodies to phospho-Akt (no. 9271S) and total-Akt (no. 9272S) were purchased from Cell Signaling Technology (Danvers, MA, USA). The antibodies to phospho-AMPK (Thr172, AA393) and  $\beta$ -actin were obtained from Beyotime (Haimen, China). The antibodies to total-AMPK (no. BM2103) and HO-1 (no. PB0212) were purchased from BOSTER Technology (Wuhan, China). HRP-goat-anti-rabbit IgG (no. MBL458) and HRP-goat-anti-mouse IgG (no. MBL 330) were purchased from MBL (Nagoya, Japan). The HO-1 inhibitor, Znpp (ALX-430-049-M025), was purchased from Enzo Life Science (Ann Arbor, MI, USA). D-4F (purity 95%) was synthesized by China Peptides Co. (Shanghai, China). 2',7'-dichlorofluorescein diacetate (DCFH-DA), dihydroethidium (DHE), LY294002 and crystal violet were purchased from Sigma-Aldrich (St. Louis, MO, USA). DMEM, trypsin and FBS were purchased from Gibco Co. (Carlsbad, CA, USA). Small interfering RNA (siRNA) specific for AMPK, HO-1, ABCA1 and scrambled control siRNA were synthesized by RiboBio (Guangzhou, China). Lipofectamine RNAiMAX (no. 13778-075) was purchased from Invitrogen (Carlsbad, CA, USA). Transwell chambers with 8- $\mu$ m-pore polycarbonate membrane were obtained from Millipore Co. (Billerica, MA, USA). Cell Counting Kit-8 (CCK-8) was purchased from Enzo Biochem Inc. (Farmingdale, NY, USA). All other

chemicals and reagents were of analytical grade and obtained from commercial sources.

### Cell culture

All animal experiment procedures were approved by the Ethics Committee of Animal Research, Xiamen University Medical College. VSMCs were isolated by collagenase digestion of the thoracic aortas from 200–250-g male Sprague Dawley rats as previously described [20]. VSMCs were grown in DMEM media supplemented with 10% FBS and antibiotics (100 units/ml of penicillin, 100  $\mu$ g/ml of streptomycin) at 37°C and maintained in an atmosphere of 5% CO<sub>2</sub>. VSMCs were identified using immunofluorescence with a specific monoclonal anti- $\alpha$ -actin antibody. Cells at passages 4–6 were used for further experiments.

### Isolation and oxidation of LDL

LDL was isolated by ultracentrifugation, as described previously [21]. Briefly, human plasma density was adjusted to 1.3 g/ml with KBr. Saline (1.006 g/ml) was layered over plasma to form a discontinuous NaCl/KBr density gradient. The samples were centrifuged at 350,000 g for 4 hrs at 4°C. LDL was collected, dialysed, sterilized and stored at 4°C in the dark. Ox-LDL was prepared via exposure of LDL to 5  $\mu$ M of CuSO<sub>4</sub> for 24 hrs at 37°C [20]. The oxidation was terminated by EDTA-Na<sub>2</sub> (1 mg/ml), and lipoprotein was further dialysed with PBS for 48 hrs. Ox-LDL was sterilized again for cell culture. All recruited healthy volunteers had written the informed consent.

### Cell proliferation assay

VSMC proliferation was evaluated by CCK-8 cell viability assay following the manufacturer's instructions. Briefly, VSMCs were seeded at  $6 \times 10^4$  cells/well in 96-well plates. After 70–80% confluence, VSMCs were starved with FBS-free DMEM media for additional 8 hrs. VSMCs were pre-treated with or without D-4F (20  $\mu$ g/ml) for 8 hrs and then induced by ox-LDL (100  $\mu$ g/ml) for 24 hrs to stimulate cell proliferation. A volume of 10  $\mu$ l of CCK-8 reagent was added to each well, and cells were further incubated for 2 hrs at 37°C. The absorbance was read at 450 nm using a spectrophotometric plate reader.

### Transwell migration assay

Cell migration was determined using a 24-well transwell plate containing polycarbonate 8- $\mu$ m-pore membrane filters. VSMCs mixed with or without D-4F (20  $\mu$ g/ml) were seeded in the upper wells ( $1 \times 10^6$  cells per 200  $\mu$ l of FBS-free DMEM media), whereas the lower wells were filled with 800  $\mu$ l of DMEM media containing 10% FBS. After 8 hrs, ox-LDL (100  $\mu$ g/ml) was added to each chamber. Cells were allowed to migrate across the porous filters for 6 hrs at 37°C. VSMCs were fixed with 4% paraformaldehyde in PBS and stained with crystal violet. The number of cells that had migrated to the lower side of the filter was counted in six random fields (100 $\times$ ) per well using light microscopy (Nikon, Tokyo, Japan).

## Scratch-wound assay

VSMCs were grown to 80% confluence in 6-well plates, and the monolayer cells were scratched gently. Cells were rinsed twice with PBS to remove cellular debris, and the linear wound was recorded. VSMCs were starved for 8 hrs and then pre-incubated with or without D-4F (20  $\mu$ g/ml) for 8 hrs in FBS-free DMEM media. Subsequently, cells were induced with ox-LDL (100  $\mu$ g/ml) for 24 hrs. The number of cells that migrated into the wound space was manually counted in six random fields (100 $\times$ ) per well using light microscopy.

## Measurement of intracellular ROS in VSMCs

Intracellular ROS levels were detected using the oxidant-sensitive probe 2',7'-dichlorofluorescein diacetate (DCFH-DA), as described previously [22]. VSMCs were grown on glass cover slips in 35-mm dishes at  $1 \times 10^4$  cells/well and cultured in DMEM media with 10% FBS. VSMCs were starved with FBS-free DMEM media for 8 hrs and pre-incubated in the absence or presence of 5  $\mu$ M of Znpp for 2 hrs. Then cells were treated with D-4F (20  $\mu$ g/ml) for 8 hrs. Subsequently, cells were washed twice with PBS and incubated with 5  $\mu$ M of DCFH-DA for 30 min. VSMCs were further incubated with ox-LDL (100  $\mu$ g/ml) for 15 min. The relative DCF fluorescence intensity was detected by fluorescent microscopy (Nikon). The excitation wavelength was 480 nm and the emission wavelength was 530 nm for DCF. The fluorescence intensity of the stained cells was determined using Image-Pro Plus/IOD.

## siRNA transfection

AMPK, HO-1 and ABCA1 siRNA transfection was performed as described previously [21]. VSMCs were seeded in 6-well plates ( $1 \times 10^6$  cells/well). At 30–50% confluence, VSMCs were transfected with 100 nM of AMPK siRNA, HO-1 siRNA, ABCA1 siRNA or scrambled siRNA in Opti-MEM with Lipofectamine RNAiMAX. After transfection for 6 hrs, the media was replaced by DMEM with 10% FBS. After 48 hrs of culture and following 8 hrs of serum deprivation, VSMCs were incubated with 20  $\mu$ g/ml of D-4F for 15 min to detect Akt and AMPK phosphorylation and for 8 hrs to assay HO-1 expression.

## Western blot

Proteins were separated by 10% or 12% SDS-PAGE and blotted onto a polyvinylidene difluoride membrane. The specific immunoreactive blots were detected by electrochemiluminescence and analysed using Quantity One 1-D Analysis Software (Bio-Rad, Hercules, CA, USA).

## Rat artery intima hyperplasia model

Male Sprague Dawley rats (300–350 g) were provided by the Experimental Animal Center of Xiamen University and randomly divided into four groups: (i) sham group ( $n = 10$ ), (ii) PBS group with injury surgery ( $n = 10$ ), (iii) D-4F group with injury surgery ( $n = 10$ ) and (iv) Znpp plus D-4F group with injury surgery ( $n = 10$ ). D-4F (1 mg/kg body weight) was administered intragastrically starting 2 days prior to

carotid injury daily and continued until the end of study. In addition, rats in Znpp plus D-4F group were injected intraperitoneally with Znpp (10 mg/kg body weight) daily 1 hrs before D-4F treatment, and rats in the other groups were injected with DMSO similarly. Rats were anesthetized by intraperitoneal injection of sodium pentobarbital (80 mg/kg of body weight), and the left common carotid artery was injured with a 1.5F Fogarty balloon catheter inserted to left external carotid artery via an arteriotomy incision [23]. All animal protocols were approved by the Animal Research Committee of the Xiamen University Medical College.

## Assay of histomorphometry and immunohistochemistry

The vessels were harvested 14 days after injury. Carotid arteries were embedded in OCT compound. Serial 5- $\mu$ m sections were produced for morphometric analysis. The sections were stained with haematoxylin and eosin (H&E) for neointimal formation analysis. To detect vessel ROS production, the sections were incubated at 37°C for 30 min in a light-protected humidified chamber with KREBS (118 mM NaCl, 4.65 mM KCl, 1.18 mM MgSO<sub>4</sub>, 1.18 mM KH<sub>2</sub>PO<sub>4</sub>, 2.5 mM NaHCO<sub>3</sub>, 5.5 mM D-glucose and 0.026 mM EDTA-Na<sub>2</sub>) pH 7.4 containing 2  $\mu$ M of dihydroethidium (DHE) [24]. DHE-derived oxidation product formation was assessed using an inverted fluorescent microscope (Olympus IX71) with a 585-nm filter (excitation wavelength 488 nm; emission wavelength 610 nm). To determine the inflammatory cell infiltration, CD18 and F4/80 expression in neointima was determined by immunohistochemistry.

## Statistical analysis

All experiments were repeated at least three to four times. Differences were compared with two-tailed Student's *t*-test or one-way ANOVA using GraphPad Prism (5.0) software (La Jolla, CA, USA). Data are expressed as mean  $\pm$  S.E.M. *P*-value less than 0.05 ( $P < 0.05$ ) was considered statistically significant (\* $P < 0.05$ , \*\* $P < 0.01$ , \*\*\* $P < 0.001$ ).

## Results

### D-4F inhibited the proliferation and migration of VSMCs *in vitro*

Cell proliferation assay indicated that ox-LDL promoted VSMC proliferation; however, D-4F inhibited the proliferation of VSMCs in a dose-dependent manner *in vitro* (Fig. 1A). Consistently, transwell assays and wound-healing experiments also showed that D-4F decreased the migration of VSMCs induced by ox-LDL in a dose-dependent manner *in vitro* (Fig. 1B–E). Furthermore, we also found that D-4F had no cytotoxicity on VSMCs (Fig. S1).

### D-4F up-regulated HO-1 expression and inhibited ROS production in VSMCs

D-4F up-regulated HO-1 expression in the dose- and time-dependent manners in VSMCs (Fig. 2A and B). To investigate whether HO-1 was

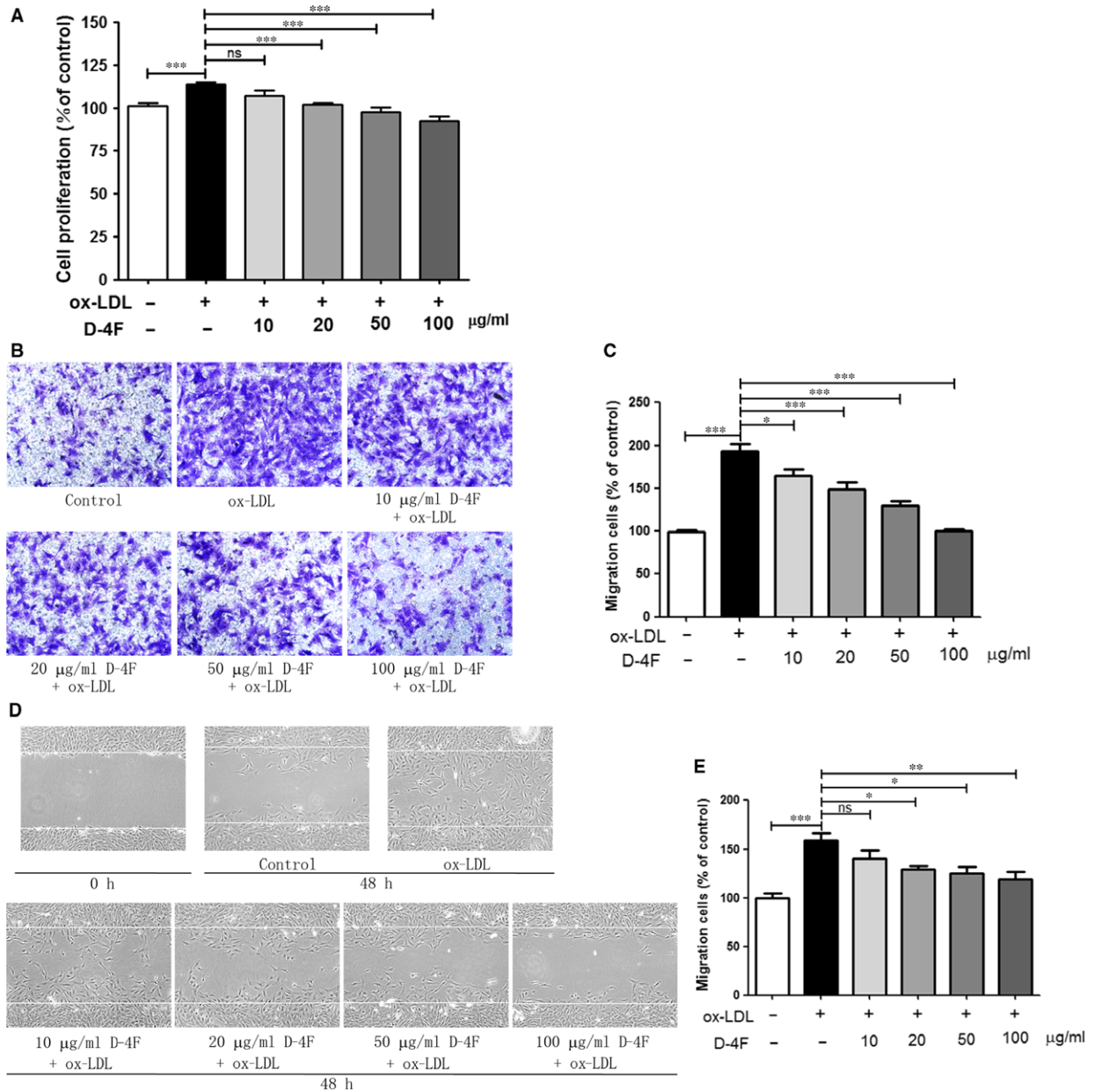


**Fig. 1** D-4F inhibited the proliferation and migration of VSMCs *in vitro*. VSMCs were pre-incubated with 10, 20, 50 or 100 μg/ml of D-4F for 8 hrs and subsequently treated with 100 μg/ml of ox-LDL for 48 hrs. Cell proliferation was evaluated by CCK-8 assay (A). Alternatively, VSMCs were treated with 100 μg/ml of ox-LDL for 8 hrs for transwell assay, and migrated cells were counted in six random fields (100×) (B and C). VSMCs were wounded by manual scraping and pre-incubated with 10, 20, 50 or 100 μg/ml of D-4F for 8 hrs and then treated with 100 μg/ml of ox-LDL for 12 hrs. Migrated cells to the scraped area were photographed and counted in six random fields (100×) (D and E). (\* $P < 0.05$ , \*\* $P < 0.01$ , \*\*\* $P < 0.001$ ).

involved in the anti-oxidative effects of D-4F, HO-1 was down-regulated through siRNA transfection (Fig. 2C). Ox-LDL triggered the prominent generation of intracellular ROS through monitoring the fluorescence intensity of DCFH-DA oxidation (Fig. 2D and E). D-4F remarkably inhibited ROS production triggered by ox-LDL in VSMCs.

However, down-regulation of HO-1 impaired the anti-oxidative effects of D-4F (Fig. 2D and E). Consistently, we also found that the HO-1 inhibitor, Znpp, effectively decreased the anti-oxidative effects of D-4F (Fig. S2 A and B). These data showed that D-4F inhibited ROS release through HO-1 up-regulation in VSMCs.

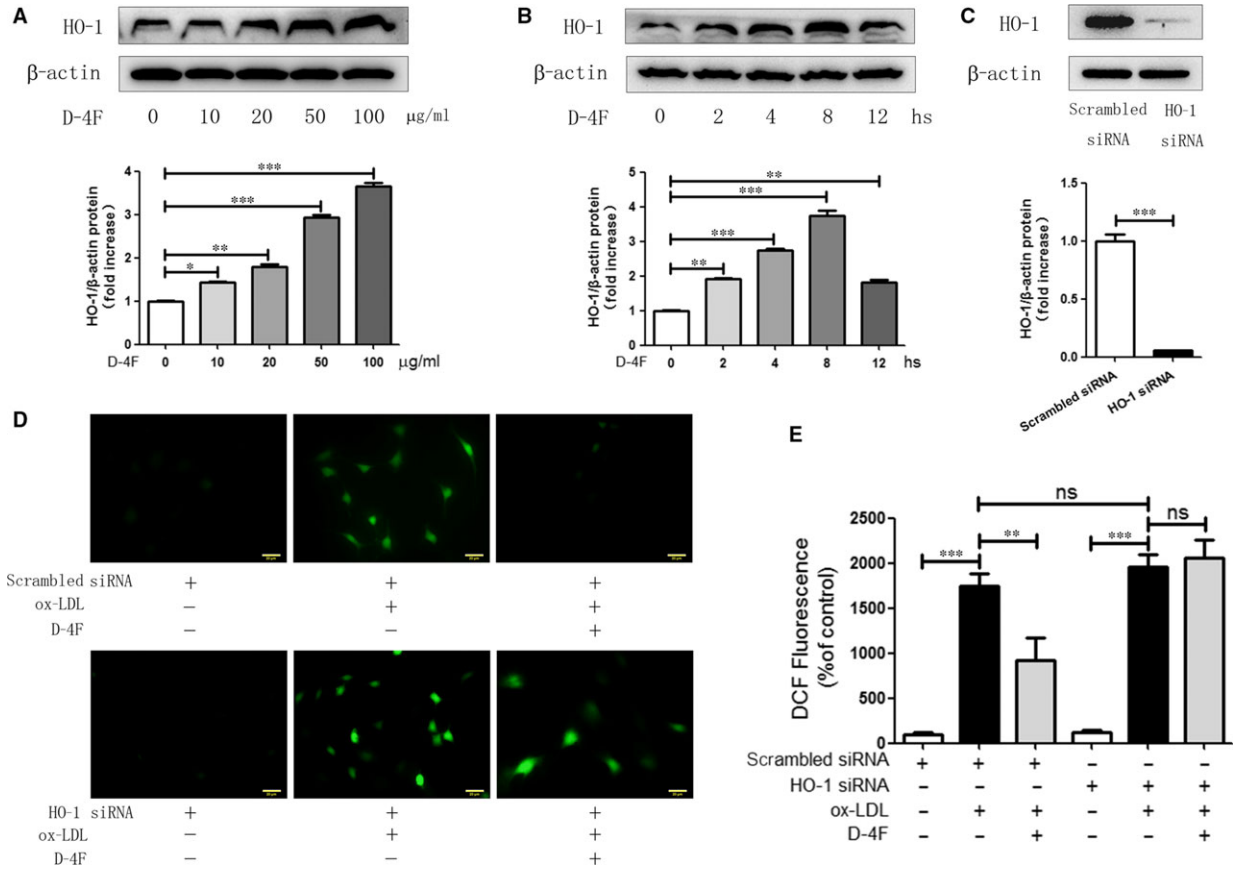


**Fig. 2** D-4F up-regulated HO-1 expression and inhibited ROS production in VSMCs. VSMCs were treated with 10, 20, 50 or 100 μg/ml of D-4F for 8 hrs or with 20 μg/ml of D-4F for 2, 4, 8 or 12 hrs. HO-1 expression was assayed by Western blot (**A** and **B**). VSMCs were transfected with scrambled siRNA or HO-1 siRNA, and the down-regulation of HO-1 was detected by Western blot (**C**). VSMCs transfected with scrambled siRNA or HO-1 siRNA were pre-treated with or without 20 μg/ml of D-4F for 8 hrs and subsequently induced by 100 μg/ml of ox-LDL for 15 min. ROS production was detected by DCF-DA fluorescence staining (400×) (**D** and **E**). The bar length was 20 micrometre. (\* $P < 0.05$ , \*\* $P < 0.01$ , \*\*\* $P < 0.001$ )

### Inhibition of HO-1 decreased the anti-proliferative and anti-migrative effects of D-4F

D-4F efficiently prevented the proliferation and migration of VSMCs induced by ox-LDL, which was similar to that in Fig. 1. However, the HO-1 inhibitor, Znpp, significantly impaired the protective functions of D-4F on VSMC proliferation and migration (Fig. 3A–E). Thus, it seems that the HO-1 pathway participated in the anti-proliferative and anti-migrative effects of D-4F on VSMCs.

### D-4F induced HO-1 expression through PI3K/Akt/AMPK pathway

Activation of Akt plays crucial roles in regulating VSMC proliferation and artery restenosis in response to injury [25]. AMP-activated protein kinase (AMPK) acts as a central regulator in the cellular redox

[26]. Therefore, the roles of Akt and AMPK in the expression of HO-1 were evaluated. D-4F triggered the phosphorylation of Akt and AMPK in VSMCs (Fig. 4A). In addition, the specific inhibitor of Akt, LY294002, inhibited the activation of AMPK, which implied that AMPK was in the downstream of Akt (Fig. 4B). Furthermore, LY294002 also inhibited HO-1 expression induced by D-4F (Fig. 4C). Additionally, silencing AMPK by siRNA transfection reduced HO-1 expression induced by D-4F (Fig. 4D and E). Therefore, it appears that D-4F promoted HO-1 up-regulation through Akt/AMPK pathway.

### D-4F induced Akt and AMPK activation and up-regulated HO-1 expression through ABCA1

To determine whether ATP-binding cassette transporter A1 (ABCA1) was involved in Akt and AMPK activation and HO-1 expression, ABCA1 was silenced in VSMCs. Down-regulation of ABCA1 eliminated

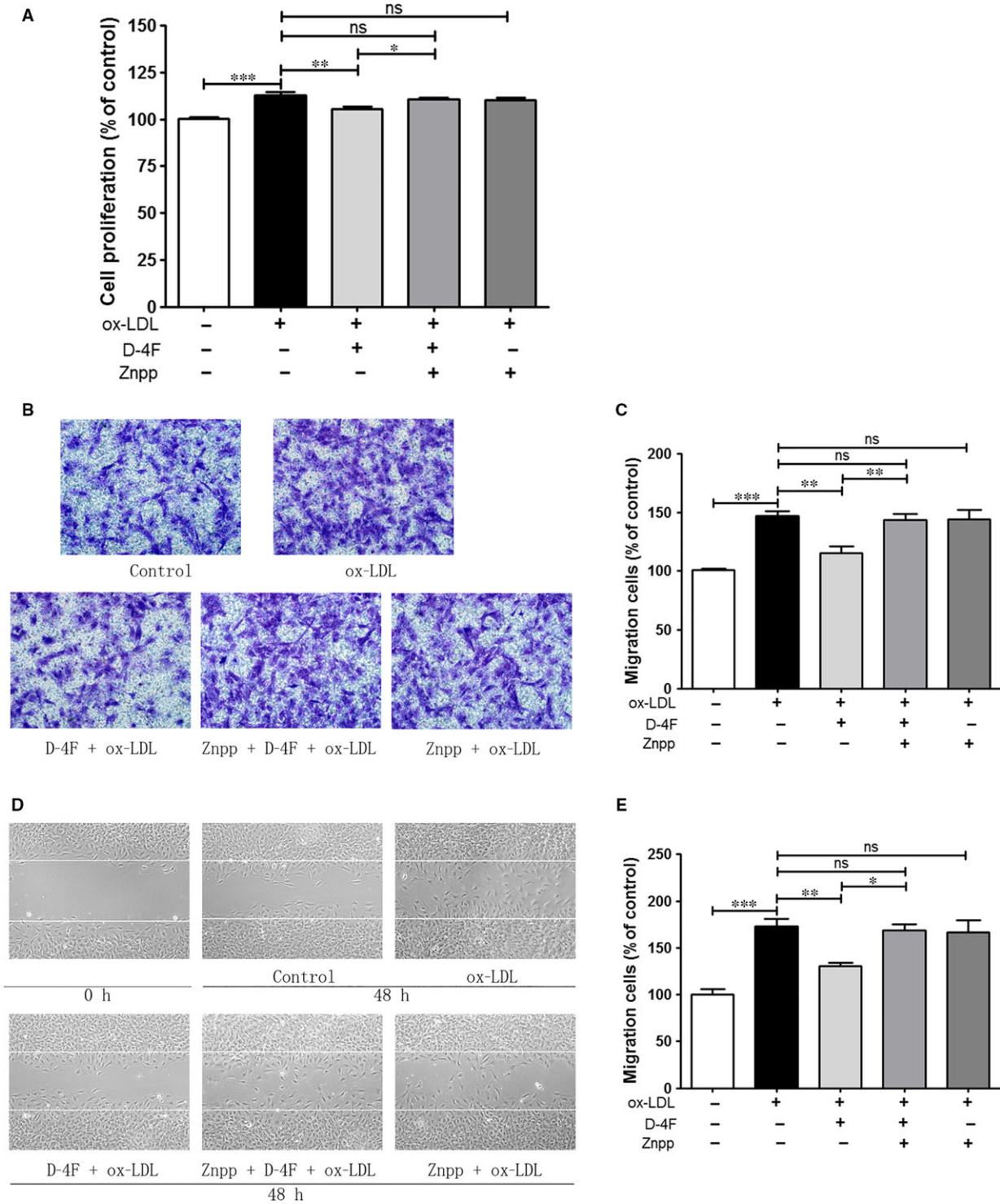


**Fig. 3** Inhibition of HO-1 decreased the anti-proliferative and anti-migrative effects of D-4F. VSMCs were pre-incubated in the presence or absence of 5  $\mu$ M of Znpp for 2 hrs and subsequently incubated with or without 20  $\mu$ g/ml of D-4F for 8 hrs. Cells were further treated with 100  $\mu$ g/ml of ox-LDL for 48 hrs for cell proliferation (A). Alternatively, after incubation with 20  $\mu$ g/ml of D-4F, VSMCs were treated with 100  $\mu$ g/ml of ox-LDL for 8 hrs for transwell migration assay (100 $\times$ ) (B) or for 12 hrs for wound-healing assay (100 $\times$ ) (D). Migrated cells were photographed and counted in six random fields (C and E). (\* $P$  < 0.05, \*\* $P$  < 0.01, \*\*\* $P$  < 0.001).

the activation of Akt and AMPK, and meanwhile, inhibited the up-regulation of HO-1 triggered by D-4F (Fig. 5A and B). Consistently, the reduction in ROS caused by D-4F was also impaired because of ABCA1 down-regulation (Fig. 5C and D). Consequently, ABCA1 appeared to be involved in the activation of Akt and AMPK, and the expression of HO-1 induced by D-4F in VSMCs.

## D-4F alleviated neointimal formation and ROS production in carotid arteries through HO-1 *in vivo*

To investigate whether D-4F alleviated neointimal formation of arteries *in vivo* and whether HO-1 was involved in these

processes, carotid artery balloon injury was performed on Sprague Dawley rats. Fourteen days after balloon injury, arteries in D-4F-treated group exhibited slighter neointimal formation than those in control group (Fig. 6A). The intima-to-media ratio of D-4F-treated group was also lower than that of control group (Fig. 6B). However, arteries in Znpp plus D-4F-treated group displayed more severe neointimal formation than those of D-4F-treated group (Fig. 6A). Consistently, the intima-to-media ratio of Znpp plus D-4F-treated group was also higher than that of D-4F-treated group (Fig. 6B). To test whether D-4F also inhibited ROS production in vessels *in vivo*, and whether HO-1 was involved in the clearance of ROS in arteries, carotid artery sections were incubated with DHE. In the presence of ROS, DHE is oxidized to fluorescent products when they intercalate into DNA [24]. The balloon

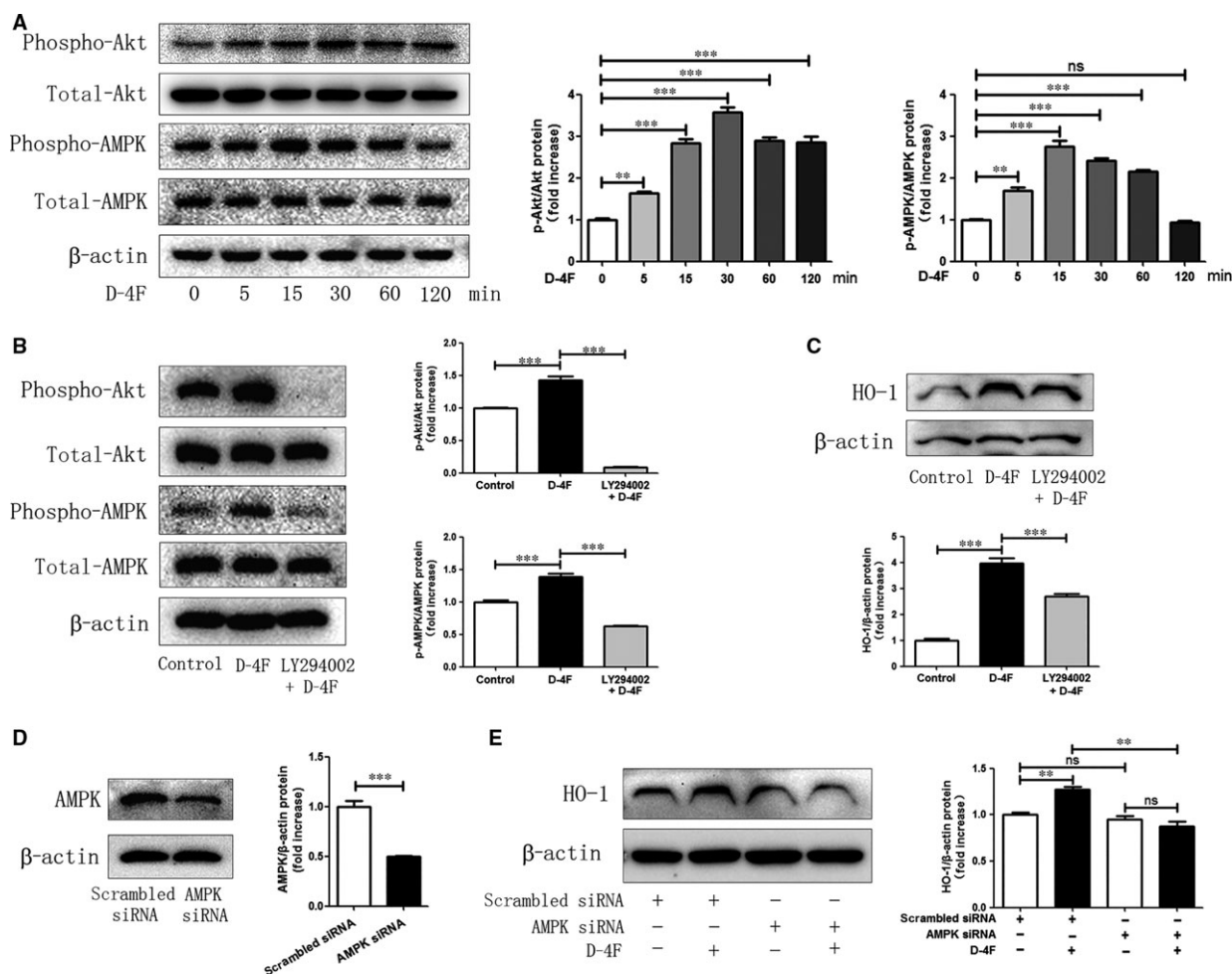


**Fig. 4** D-4F induced HO-1 expression through PI3K/Akt/AMPK pathway. VSMCs were treated with 20  $\mu\text{g/ml}$  of D-4F for 0, 5, 15, 30, 60 or 120 min, and the phosphorylation of Akt and AMPK was assayed by Western blot (**A**). VSMCs were pre-treated with the Akt inhibitor, LY294002 (20  $\mu\text{M}$ ), for 1 hr, and following incubated with D-4F (20  $\mu\text{g/ml}$ ) for 15 min to test Akt and AMPK phosphorylation or for 8 hrs to assay HO-1 expression by Western blot (**B** and **C**). Scrambled siRNA or AMPK siRNA was transfected into VSMCs for 48 hrs, and then, cells were incubated with 20  $\mu\text{g/ml}$  of D-4F for 8 hrs. Expression of AMPK and HO-1 was assayed by Western blot (**D** and **E**).

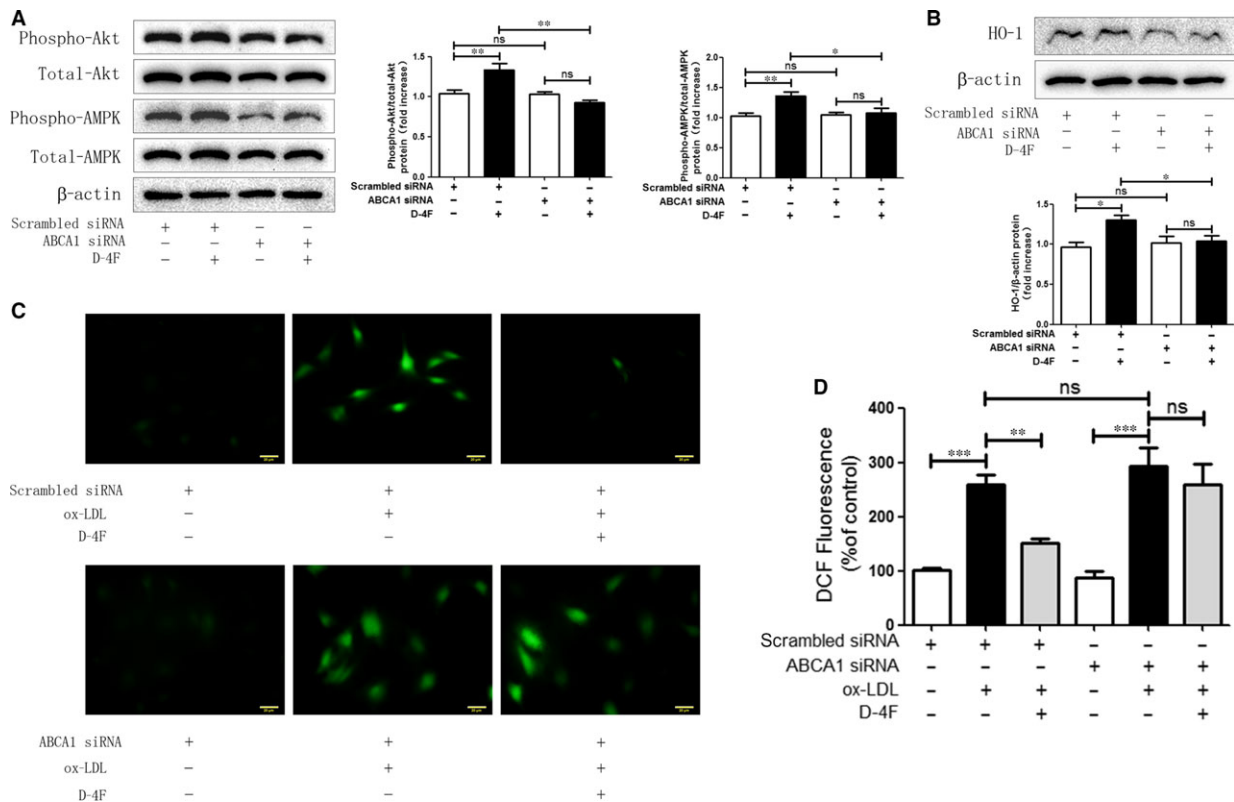


**Fig. 5** D-4F induced Akt and AMPK activation and up-regulated HO-1 expression through ABCA1. VSMCs were transfected with scrambled siRNA or ABCA1 siRNA and subsequently incubated with or without 20  $\mu$ g/ml of D-4F for further 15 min (A) or 8 hrs (B). The phosphorylation of Akt and AMPK and the expression of HO-1 were detected by Western blot (A and B). Alternatively, after siRNA transfection and incubation with D-4F, VSMCs were induced by 100  $\mu$ g/ml of ox-LDL for 15 min to assay ROS production by DCF-DA fluorescence staining (400 $\times$ ) (C and D). The bar length was 20 micrometre. (\* $P < 0.05$ , \*\* $P < 0.01$ , \*\*\* $P < 0.001$ ).

impairment mediated robust formation of DHE-derived oxidation products in carotid arteries, and arteries in D-4F-treated group showed lesser fluorescence formation than those of control group (Fig. 6C). However, arteries in Znpp plus D-4F-treated group displayed more fluorescence formation than those of D-4F-treated group (Fig. 6C). In addition, D-4F also decreased the infiltration of neutrophils and monocytes in neointima; however, arteries in Znpp plus D-4F-treated group had more inflammatory cell infiltration (Fig. S3 A and B). Thus, it seems that HO-1 also played key roles in the inhibition of ROS production, vessel inflammation and neointimal formation *in vivo*.

## Discussion

In this study, we found that D-4F up-regulated HO-1 expression and alleviated oxidative stress through PI3K/Akt/AMPK pathway in VSMCs, and ABCA1 played key roles in these processes. D-4F inhibited VSMC proliferation and migration *in vitro*, and restrained neointimal formation of carotid arteries *in vivo* through HO-1 up-regulation.

Percutaneous transluminal coronary angioplasty (PTCA) and intravascular stenting are commonly used for ASCVD treatment; however, the rates of recurrent vessel narrowing are unacceptably high even using drug-eluting stents [27]. The pathophysiology of restenosis is a process comprised of VSMC proliferation and intimal hyperplasia [28]. VSMCs proliferate and migrate to the intima, and remodel artery vessels, where oxidative stress plays crucial roles in these processes [29]. Overexpression of the subunit of NADPH oxidase (p22phox) in VSMCs significantly enhances the production of ROS, accelerates the switch from the contractile phenotype to the synthetic phenotype and promotes the proliferation and migration of VSMCs [30]. However, decreased ROS production inhibits VSMC proliferation and inflammatory cells infiltration and reduces restenosis [6, 28]. Heme triggers ROS production derived from NADPH oxidase and subsequently induces VSMC proliferation and migration [31]. Bilirubin and carbon monoxide (CO), the metabolites of heme, inhibit VSMC proliferation and migration and decrease neointimal formation [32, 33]. These results imply that heme metabolism and oxidative stress are involved in the proliferation and migration of VSMCs. HO-1 is the key enzyme of heme metabolism and plays critical roles in the anti-

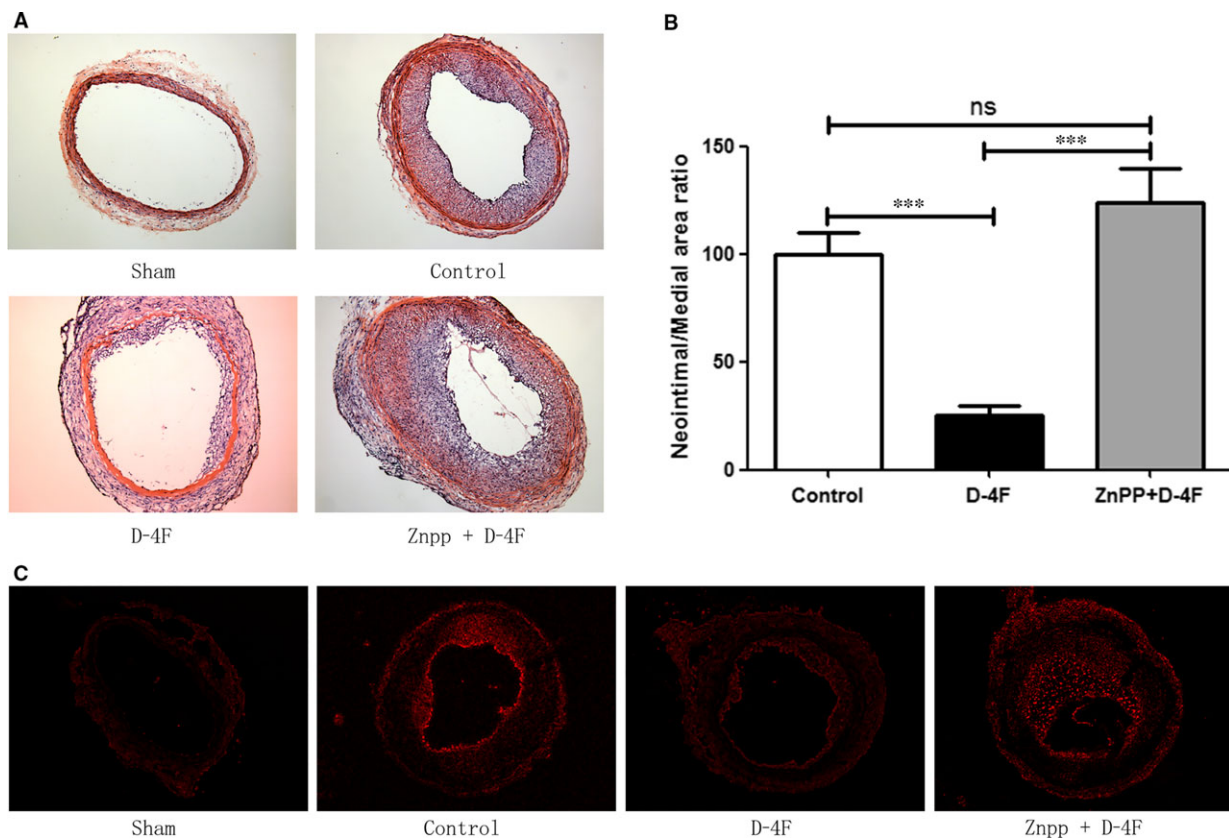


**Fig. 6** D-4F alleviated neointimal formation and ROS production of carotid arteries through HO-1 *in vivo*. Representative carotid arteries after balloon injury in Sprague Dawley rats in sham, control, D-4F and Znpp+D-4F groups were stained by haematoxylin and eosin (H&E) (4×) (A). The intima-to-media ratio of vessels was expressed as the mean ± S.E.M. in each group ( $n = 10$ ) (B). ROS generation was detected through DHE-derived fluorescent oxidation products in neointima of carotid arteries (4×) (C).

oxidance of cells [34]. This inducible enzyme is implicated in the cellular defences against oxidative stress, inflammation and apoptosis associated with atherosclerosis [34, 35]. HO-1 inhibits VSMC proliferation and migration *in vitro* and reduces intimal hyperplasia during vascular injury *in vivo* [36, 37]. Wu *et al.* also demonstrated that HDL decreases collar-induced endothelial adhesion molecule expression and reduces intima/media neutrophil infiltration by inducing HO-1 expression; however, down-regulation of HO-1 abolishes the protective effects of HDL [38]. In addition, Vanella *et al.* showed that L-4F increases adiponectin production and reverses adipocyte dysfunction via increasing HO-1 expression both *in vitro* and *in vivo* [39]. Kruger *et al.* also demonstrated that D-4F decreases endothelial cell sloughing and improves vascular reactivity through inducing HO-1 expression in diabetic rats [40]. In this study, D-4F up-regulated HO-1 expression, reduced ROS production and inhibited VSMC proliferation and migration (Figs 1 and 2). However, inhibition of HO-1 decreased the anti-oxidative functions and impaired the anti-proliferative and anti-migrative effects of D-4F both *in vitro* and *in vivo* (Figs 3 and 6, and Fig. S2). The inflammatory cells infiltrate the subendothelial layer

and subsequently release more growth factors and inflammatory cytokines, which aggravates VSMC migration and proliferation, and neointimal hyperplasia [28]. Here, we found that D-4F also inhibited inflammatory cell infiltration in the neointima through HO-1 (Fig. S3).

Activation of Akt is involved in the proliferation and migration of VSMCs [25]. HDL up-regulates HO-1 through PI3K/Akt pathway in endothelial cells [38]. AMPK is a critical energy and redox sensor, and AMPK activation ameliorates oxidative stress-associated cardiovascular disease [26, 41]. AMPK inhibits VSMC proliferation and migration, and alleviates vascular remodelling through regulating the stability of cytoskeleton and extracellular matrix (ECM) [42]. In addition, the activation of AMPK boosts HO-1 expression and promotes endothelial cell survival during oxidative stress [43]. However, down-regulation or inhibition of AMPK blunts HO-1 expression and interrupts cellular redox and energy balance [44]. In this study, D-4F induced Akt and AMPK phosphorylation in VSMCs. Inhibition of Akt decreased the activation of AMPK and the up-regulation of HO-1 induced by D-4F. Meanwhile, down-regulation of AMPK reduced HO-1 expression triggered by D-4F (Fig. 4). Therefore, it appears that D-

4F induced HO-1 expression through PI3K/Akt/AMPK pathway in VSMCs.

ABCA1 displays key roles in anti-atherosclerosis [45]. Choi *et al.* showed that reduced ABCA1 expression in VSMCs contributes to less binding of apoA-I and consequently leads to VSMC-derived foam cell formation in the intima [46]. Tabet *et al.* also reported that apoA-I mimetic peptide, 5A, protects endothelial cell from oxidative stress and inflammation through the interaction with ABCA1 [47]. We found that D-4F induced Akt and AMPK phosphorylation, up-regulated HO-1 expression and scavenged ROS via ABCA1 in VSMCs (Fig. 5). Thus, this implies that ABCA1 mediated the anti-oxidative effects of D-4F in VSMCs.

In summary, apoA-I mimetic peptide, D-4F, up-regulated HO-1 expression via PI3K/Akt/AMPK pathway. And D-4F inhibited VSMC proliferation and migration and reduced neointimal formation of carotid arteries in the HO-1-dependent manner, which might provide a novel prophylactic and therapeutic strategy for anti-restenosis of arteries after PTCA or percutaneous coronary intervention (PCI).

## Acknowledgements

This project was supported by Grants 31200884, 81270294 and 91129713 from the National Natural Science Foundation of China; by Grants 2016D016 and 2016-ZQN-92 from the Natural Science Foundation of Fujian; and by Grants 3502Z20154048, 3502Z20144061 and 2014279 from the Natural Science Foundation of Xiamen.

## References

1. Weber C, Noels H. Atherosclerosis: current pathogenesis and therapeutic options. *Nat Med.* 2011; 17: 1410–22.
2. Doran AC, Meller N, McNamara CA. Role of smooth muscle cells in the initiation and early progression of atherosclerosis. *Arterioscler Thromb Vasc Biol.* 2008; 28: 812–9.
3. Johnson JL. Emerging regulators of vascular smooth muscle cell function in the development and progression of atherosclerosis. *Cardiovasc Res.* 2014; 103: 452–60.
4. Chistiakov DA, Orekhov AN, Bobryshev YV. Vascular smooth muscle cell in atherosclerosis. *Acta Physiol (Oxf).* 2015; 214: 33–50.
5. Brown DI, Griendling KK. Regulation of signal transduction by reactive oxygen species in the cardiovascular system. *Circ Res.* 2015; 116: 531–49.
6. Clempus RE, Griendling KK. Reactive oxygen species signaling in vascular smooth muscle cells. *Cardiovasc Res.* 2006; 71: 216–25.
7. Yaghini FA, Song CY, Lavrentyev EN, *et al.* Angiotensin II-induced Vascular Smooth Muscle Cell Migration and Growth Are Mediated by Cytochrome P450 1B1-dependent Superoxide Generation. *Hypertension.* 2010; 55: 1461–7.
8. Luo X, Xiao Y, Song F, *et al.* Increased plasma S-adenosyl-homocysteine levels induce the proliferation and migration of VSMCs through an oxidative stress-ERK1/2 pathway in apoE<sup>-/-</sup> mice. *Cardiovasc Res.* 2012; 95: 241–50.
9. Wang J-N, Shi N, Chen S-Y. Manganese superoxide dismutase inhibits neointima formation through attenuation of migration and proliferation of vascular smooth muscle cells. *Free Radic Biol Med.* 2012; 52: 173–81.
10. Santilli F, D'Ardes D, Davi G. Oxidative stress in chronic vascular disease: from prediction to prevention. *Vascul Pharmacol.* 2015; 74: 23–37.
11. Feig JE, Hewing B, Smith JD, *et al.* High-density lipoprotein and atherosclerosis regression: evidence from preclinical and clinical studies. *Circ Res.* 2014; 114: 205–13.
12. van der Vorst EP, Vanags LZ, Dunn LL, *et al.* High-density lipoproteins suppress chemokine expression and proliferation in human vascular smooth muscle cells. *FASEB J.* 2013; 27: 1413–25.
13. Sun L, Ishida T, Okada T, *et al.* Expression of Endothelial Lipase Correlates with the Size of Neointima in a Murine Model of Vascular Remodeling. *J Atheroscler Thromb.* 2012; 19: 1110–27.
14. Reimers GJ, Jackson CL, Rickards J, *et al.* Inhibition of rupture of established atherosclerotic plaques by treatment with apolipoprotein A-I. *Cardiovasc Res.* 2011; 91: 37–44.
15. Navab M, Shechter I, Anantharamaiah GM, *et al.* Structure and function of HDL mimetics. *Arterioscler Thromb Vasc Biol.* 2010; 30: 164–8.
16. Ou ZJ, Li L, Liao XL, *et al.* Apolipoprotein A-I mimetic peptide inhibits atherosclerosis by altering plasma metabolites in hypercholesterolemia. *Am J Physiol Endocrinol Metab.* 2012; 303: E683–94.
17. Baotic I, Ge ZD, Sedlic F, *et al.* Apolipoprotein A-1 mimetic D-4F enhances isoflurane-induced eNOS signaling and cardioprotection during acute hyperglycemia. *Am J Physiol Heart Circ Physiol.* 2013; 305: H219–27.

## Conflict of interests

The authors confirm that there are no conflict of interests.

## Supporting information

Additional Supporting Information may be found online in the supporting information tab for this article:

**Figure S1** D-4F had no cytotoxicity on VSMCs. VSMCs were incubated with 0, 5, 10, 20, 50 and 100 µg/ml of D-4F for 12 hours. Lactate dehydrogenase (LDH) activity in the media was measured.

**Figure S2** HO-1 inhibitor, Znpp, reduced the anti-oxidant effects of D-4F. VSMCs were preincubated in the presence or absence of 5 µM of Znpp for 2 hrs, and subsequently incubated with or without 20 µg/ml of D-4F for 8 hrs. Cells were further treated with 100 µg/ml of ox-LDL for 15 min. ROS production was detected by DCF-DA fluorescence staining (400×). (\**P* < 0.05, \*\**P* < 0.01, \*\*\**P* < 0.001).

**Figure S3** D-4F inhibited the infiltration of neutrophils and monocytes in neointima through HO-1. Representative micrographs with immunohistochemical staining for CD18 (A) and F4/80 (B) of carotid artery sections in control, D-4F, and Znpp+D-4F groups were shown (200×).

18. **Ding Y, Wang Y, Zhou J, et al.** Direct cytosolic siRNA delivery by reconstituted high density lipoprotein for target-specific therapy of tumor angiogenesis. *Biomaterials*. 2014; 35: 7214–27.
19. **Du L, Qu X, Zheng H, et al.** Reverse Apolipoprotein A-I Mimetic Peptide R-D4F Inhibits Neointimal Formation following Carotid Artery Ligation in Mice. *Am J Pathol*. 2013; 182: 1932–9.
20. **Wang Y, Ji L, Jiang R, et al.** Oxidized high-density lipoprotein induces the proliferation and migration of vascular smooth muscle cells by promoting the production of ROS. *J Atheroscler Thromb*. 2014; 21: 204–16.
21. **Liu D, Ji L, Tong X, et al.** Human apolipoprotein A-I induces cyclooxygenase-2 expression and prostaglandin I-2 release in endothelial cells through ATP-binding cassette transporter A1. *Am J Physiol Cell Physiol*. 2011; 301: C739–48.
22. **Shimizu H, Hirose Y, Nishijima F, et al.** ROS and PDGF-beta receptors are critically involved in indoxyl sulfate actions that promote vascular smooth muscle cell proliferation and migration. *Am J Physiol Cell Physiol*. 2009; 297: C389–96.
23. **Jia S, Chen Z, Li J, et al.** FAM3A promotes vascular smooth muscle cell proliferation and migration and exacerbates neointima formation in rat artery after balloon injury. *J Mol Cell Cardiol*. 2014; 74: 173–82.
24. **Nobecourt E, Tabet F, Lambert G, et al.** Nonenzymatic glycation impairs the anti-inflammatory properties of apolipoprotein A-I. *Arterioscler Thromb Vasc Biol*. 2010; 30: 766–72.
25. **Choi KH, Kim JE, Song NR, et al.** Phosphoinositide 3-kinase is a novel target of piceatannol for inhibiting PDGF-BB-induced proliferation and migration in human aortic smooth muscle cells. *Cardiovasc Res*. 2010; 85: 836–44.
26. **Zimmermann K, Baldinger J, Mayerhofer B, et al.** Activated AMPK boosts the Nrf2/HO-1 signaling axis-A role for the unfolded protein response. *Free Radic Biol Med*. 2015; 88: 417–26.
27. **Goel SA, Guo LW, Liu B, et al.** Mechanisms of post-intervention arterial remodelling. *Cardiovasc Res*. 2012; 96: 363–71.
28. **Yin K, Agrawal DK.** High-density lipoprotein: a novel target for antirestenosis therapy. *Clin Transl Sci*. 2014; 7: 500–11.
29. **Satoh K, Nigro P, Berk BC.** Oxidative stress and vascular smooth muscle cell growth: a mechanistic linkage by cyclophilin A. *Antioxid Redox Signal*. 2010; 12: 675–82.
30. **Sung HJ, Eskin SG, Sakurai Y, et al.** Oxidative stress produced with cell migration increases synthetic phenotype of vascular smooth muscle cells. *Ann Biomed Eng*. 2005; 33: 1546–54.
31. **Moraes J, Barcellos-de-Souza P, Rodrigues G, et al.** Heme modulates smooth muscle cell proliferation and migration via NADPH oxidase: a counter-regulatory role for heme oxygenase system. *Atherosclerosis*. 2012; 224: 394–400.
32. **Nakao A, Murase N, Ho C, et al.** Biliverdin administration prevents the formation of intimal hyperplasia induced by vascular injury. *Circulation*. 2005; 112: 587–91.
33. **Duckles H, Boycott HE, Al-Owais MM, et al.** Heme oxygenase-1 regulates cell proliferation via carbon monoxide-mediated inhibition of T-type Ca<sup>2+</sup> channels. *Pflugers Arch*. 2015; 467: 415–27.
34. **Dunn LL, Midwinter RG, Ni J, et al.** New insights into intracellular locations and functions of heme oxygenase-1. *Antioxid Redox Signal*. 2014; 20: 1723–42.
35. **Zhao Y, Zhang L, Qiao Y, et al.** Heme oxygenase-1 prevents cardiac dysfunction in streptozotocin-diabetic mice by reducing inflammation, oxidative stress, apoptosis and enhancing autophagy. *PLoS ONE*. 2013; 8: e75927.
36. **Duckers HJ, Boehm M, True AL, et al.** Heme oxygenase-1 protects against vascular constriction and proliferation. *Nat Med*. 2001; 7: 693–8.
37. **Cheng C, Haasdijk RA, Tempel D, et al.** PDGF-induced migration of vascular smooth muscle cells is inhibited by heme oxygenase-1 via VEGFR2 upregulation and subsequent assembly of inactive VEGFR2/PDGFRbeta heterodimers. *Arterioscler Thromb Vasc Biol*. 2012; 32: 1289–98.
38. **Wu BJ, Chen K, Shrestha S, et al.** High-Density Lipoproteins Inhibit Vascular Endothelial Inflammation by Increasing  $\beta$ -Hydroxysteroid- $\Delta$ 24 Reductase Expression and Inducing Heme Oxygenase-1. *Circ Res*. 2013; 112: 278–88.
39. **Vanella L, Li M, Kim D, et al.** ApoA1: mimetic peptide reverses adipocyte dysfunction *in vivo* and *in vitro* via an increase in heme oxygenase (HO-1) and Wnt10b. *Cell Cycle*. 2012; 11: 706–14.
40. **Kruger AL, Peterson S, Turkseven S, et al.** D-4F induces heme oxygenase-1 and extracellular superoxide dismutase, decreases endothelial cell sloughing, and improves vascular reactivity in rat model of diabetes. *Circulation*. 2005; 111: 3126–34.
41. **Shirwany NA, Zou MH.** AMPK: a cellular metabolic and redox sensor. A minireview. *Front Biosci*. 2014; 19: 447–74.
42. **Stone JD, Narine A, Shaver PR, et al.** AMP-activated protein kinase inhibits vascular smooth muscle cell proliferation and migration and vascular remodeling following injury. *Am J Physiol Heart Circ Physiol*. 2013; 304: H369–81.
43. **Li FY, Lam KS, Tse HF, et al.** Endothelium-selective activation of AMP-activated protein kinase prevents diabetes mellitus-induced impairment in vascular function and reendothelialization via induction of heme oxygenase-1 in mice. *Circulation*. 2012; 126: 1267–77.
44. **Liu XM, Peyton KJ, Shebib AR, et al.** Activation of AMPK stimulates heme oxygenase-1 gene expression and human endothelial cell survival. *Am J Physiol Heart Circ Physiol*. 2011; 300: H84–93.
45. **Westerterp M, Bochem AE, Yvan-Charvet L, et al.** ATP-binding cassette transporters, atherosclerosis, and inflammation. *Circ Res*. 2014; 114: 157–70.
46. **Choi HY, Rahmani M, Wong BW, et al.** ATP-Binding Cassette Transporter A1 Expression and Apolipoprotein A-I Binding Are Impaired in Intima-Type Arterial Smooth Muscle Cells. *Circulation*. 2009; 119: 3223–31.
47. **Tabet F, Remaley AT, Segaliny AI, et al.** The 5A Apolipoprotein A-I Mimetic Peptide Displays Antiinflammatory and Antioxidant Properties *In Vivo* and *In Vitro*. *Arterioscler Thromb Vasc Biol*. 2010; 30: 246–52.